

Cancer Cell

Metastasis Suppressor Aes Inhibits Notch Signaling

associated and colocalized with Aes in the nuclear foci (Figure S4). Collectively, these results suggest that Aes, together with TLE1, can hold the Rbpj/NICD/Maml1 complex in nuclear foci where transcription is repressed.

Notch Signaling Inhibition Can Suppress Metastasis

Above results also suggested that Aes suppressed metastasis through inhibition of Notch signaling. As anticipated, attenuation of the signaling by constitutive expression of shRNA constructs against *RBPJ* mRNA (*shRBPJ*) suppressed metastasis of HCA7 human colon cancer cells from the rectum to liver (multiplicity; 6.0 ± 2.7 versus 2.6 ± 1.6 , $p = 0.02$) and to lungs (341 ± 89 versus 87 ± 40 , $p < 0.01$) (Figures 5A and 5B) in nude mice. We obtained similar results also with mouse Colon26 cells expressing a dominant-negative mutant of Rbpj (*dnRbpj*; R218H; Kato et al., 1997) (Figures S5A and S5B). We then tested inhibition of Notch signaling with Compound E, a potent γ -secretase inhibitor (Milano et al., 2004; Schmidt, 2003; Zaczek et al., 1999) (GSI) (Figure 5C). It significantly suppressed metastasis of Colon26 cells to the liver (5.7 ± 5.5 versus 1.8 ± 2.4 , $p = 0.04$) and lungs (54 ± 22 versus 18 ± 8 , $p < 0.01$) (Figure 5D) from the rectum. Importantly, none of *shRBPJ*, *dnRbpj*, or Compound E affected the size of primary tumors significantly (Figures S5C–S5E). Likewise, Compound E had little effect on the primary Colon26 tumors regarding their differentiation and proliferation (Figures S5F and S5G). These results underscore that Notch signaling plays an essential role in hematogenous metastasis of colon cancer cells.

Notch Activation by Stromal Ligands Induces Tumor Intravasation

Using immunofluorescence staining, we found that mouse Colon26 cells expressed abundant Notch1 receptor (Figure 6A, left), consistent with a report on human colon cancer (Zagouras et al., 1995). Notably, there was much Jagged1 ligand on the blood vessels in primary tumors (Figure 6A) as well as in their metastases to the liver (Figure 6B) and lungs (Figure 6C, left). Jagged1 was expressed also on normal epithelial cells in these organs (Figure 6B, Lv; hepatocytes: Figure 6C, right, Lg; pneumocytes expressing TTF-1). We also found that blood vessels and macrophages expressed another Notch ligand Delta-like 4 (Dll4) (Figures S6A–S6C). Curiously, activated NICD was detected in the tumor epithelium that was surrounded by DLL4-expressing stromal cells in human colon cancer tissues (Figure 6D). We employed the Q scoring (Detre et al., 1995), and obtained Spearman's correlation factor of 0.69, indicating a very strong association (0.6–0.8) between DLL4 and NICD expression ($p < 0.01$).

To test whether ligand-expressing stromal cells activated Notch signaling in cancer cells, we constructed "Notch reporter Colon26 (C26^{RBS-EGFP}) cells" that contained RBS (Rbpj binding sequence)-EGFP reporter, expressing EGFP upon Notch signal activation (Figure 6E). As expected, expression of RAMIC induced EGFP in the reporter cells in culture (Figure 6F). Convincingly, the EGFP staining was strongest in the C26^{RBS-EGFP} cells located around blood vessels of the primary tumor in the Balb/c rectum (Figure 6G, left). Treatment of the tumor-bearing mice with Compound E, as well as overexpression of Aes in the reporter cells, almost eliminated expression of EGFP (Figure 6G, center and right), supporting that Aes acts through

suppression of the Notch signaling. Interestingly, we found expression of EGFP in two types of metastasized cell clusters in the lung; micrometastases consisting of only a few cancer cells (Figure 6H, left), and cells at the periphery of larger metastases that were expanding in the lung parenchyma (Figure 6H, right) (see Discussion).

Because Aes was downregulated in cancer cells adjoining blood vessels (Figure 1E, bottom), we hypothesized that loss of Aes expression stimulated transendothelial migration (TEM) through Notch signal activation. To test the hypothesis in vitro, we placed cancer cells on a layer of HUVEC (human umbilical vein endothelial cells) that expressed Notch ligands (Lu et al., 2007; Mailhos et al., 2001). As expected, knocking down Aes in Colon26 cells stimulated HUVEC-induced Notch signaling as determined by Q-RT-PCR of *Hes1* mRNA (Figure 6I) and enhanced their TEM through the HUVEC layer (Figure 6J). Similar results were obtained with HCA7 cells (Figure S6D). Notably, expression of *shRBPJs* inhibited Notch signaling that was triggered by HUVEC (Figure 6K) and reduced their TEM significantly (Figure 6L). To observe TEM more dynamically, we took time-lapse movies of Colon26 cells with or without Aes induction migrating through the HUVEC cell layer (Movie S1). While approximately two-thirds of control Colon26 cells migrated underneath the HUVEC layer in 12 hr, only approximately one-third of the Aes-overexpressing Colon26 cells did (Figure S6E). We also found that recombinant DLL4 and JAGGED1 activated Notch signaling and enhanced motility of Colon26 cells when analyzed by simpler scratch assays (Figure S6F). These results are consistent with our hypothesis that Aes suppresses metastasis of colon cancer cells by inhibition of Notch signaling that stimulates cancer cell motility and TEM at the steps of local invasion, intravasation, and extravasation (see Discussion).

Aes Knockout Causes Tumor Intravasation

To test above hypothesis with endogenous tumors, we constructed a floxed allele of Aes (*Aes^f*), and introduced it into the *Apc^{Δ716}* intestinal polyposis model carrying villin-Cre^{ERT2} transgene (*TgvCre^{ERT2}*) (el Marjou et al., 2004) whose tumors expressed substantial amounts of Aes (Figures 7A and 7B; Figures S7A and S7B). At 3 weeks of age, we treated the compound mutant *Apc^{+/Δ716}-Aes^{f/f}-TgvCre^{ERT2}* with 4-hydroxytamoxifen (4HT) to activate Cre recombinase in the intestinal epithelium, generating *Apc^{+/Δ716}-Aes^{Δex2/Δex2}-TgvCre^{ERT2}* genotype (*Apc/Aes*). In these mice that had lost Aes exon 2 (Figure S7C), we found marked tumor invasion and intravasation into the smooth muscle layer of the small intestine and colon (Figures 7D and 7E; *Apc/Aes*). Although all *Apc/Aes* mutants (25 examined) showed this invasion phenotype at 17 weeks of age, *Apc^{Δ716}* polyposis mice never did (Kitamura et al., 2007; Oshima et al., 1995; Takaku et al., 1998) (Figure 7C; *Apc*). For the *Apc/Aes* polyps larger than 2 mm in diameter, about half of them was found invading into the submucosa or beyond (Figure 7F).

Strikingly, many of the invading tumor glands in the *Apc/Aes* mice were found inside vessels that were often distended, reminiscent of tumor embolism (Figure 7G, left). This intravasation was further confirmed by immunofluorescence for epithelial marker cytokeratin and vessel marker CD31 or blood vessel marker VE-cadherin (Figure 7G, center and right, respectively). Although such intravasating tumor epithelial cells should be

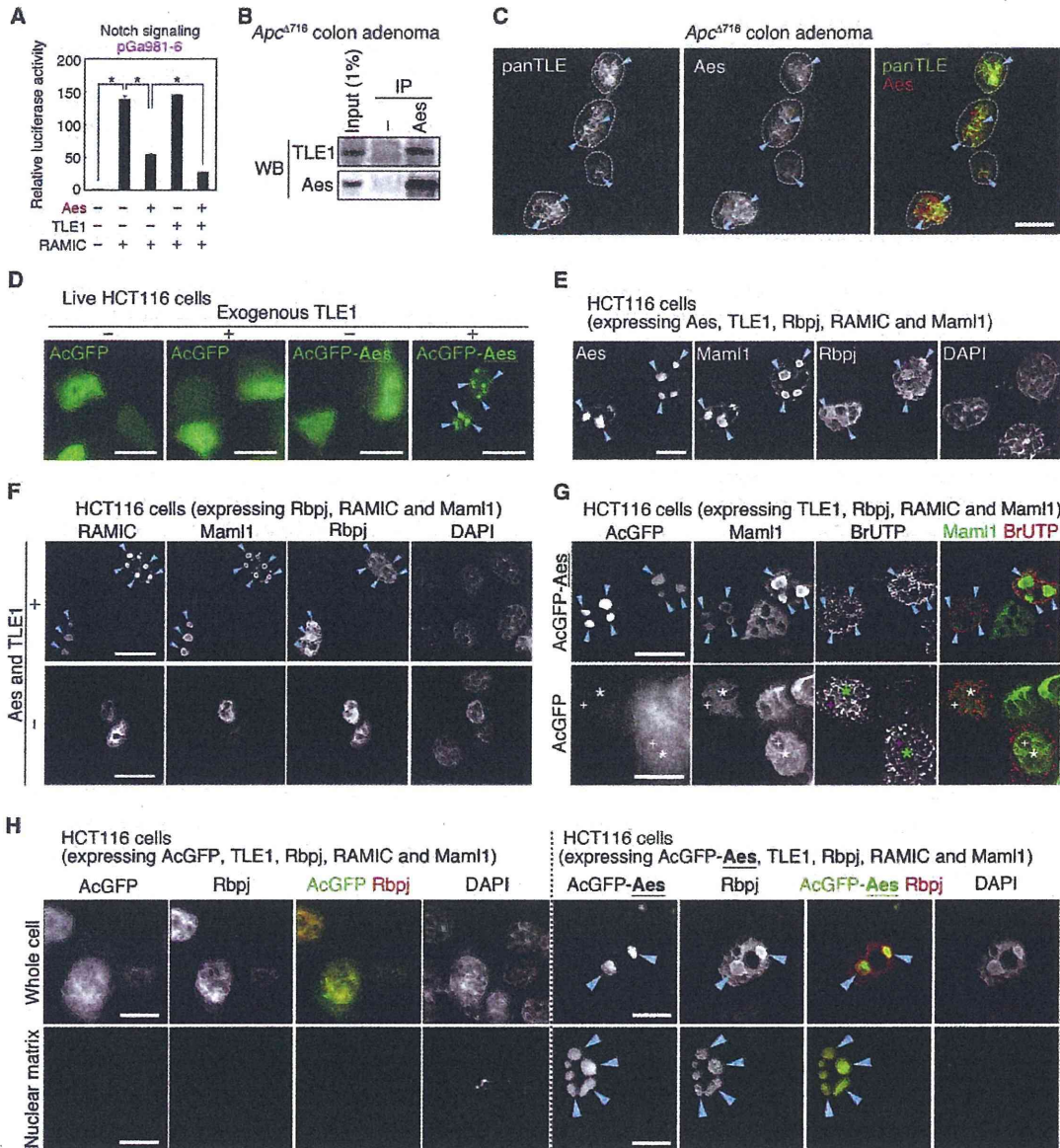


Figure 4. Colocalization of Aes and TLE1 with Notch Pathway Proteins in Nuclear Foci

(A) Effects of overexpression of Aes and TLE1 on RAMIC-induced Notch signaling determined by pGa981-6 luciferase reporter in HEK293 cells. **p* < 0.01. Error bars indicate SD (*n* = 3).

(B) In vivo interaction between endogenous Aes and TLE1 in colonic adenomas of *Apc*^{Δ716} mice. Aes in the tumor lysates was immunoprecipitated (IP) using anti-Aes antibody. Subsequently, Aes and TLE1 in the precipitates were detected by western blotting (WB).

(C) Immunofluorescence of endogenous TLE and Aes in an *Apc*^{Δ716} colon adenoma. TLE proteins were detected by anti-panTLE antibody that had been raised against WD repeats. Arrowheads indicate colocalization of TLE and Aes in the nucleus (circled by broken lines). Scale bar, 10 μm.

(D) Effects of TLE1 overexpression on localization of Aes. HCT116 cells were transfected with expression plasmids for AcGFP or AcGFP-Aes simultaneously with or without TLE1. Twenty-four hours after transfection, localization of AcGFP in live cells was analyzed under a fluorescent microscope. Scale bars, 10 μm.

(E) Immunofluorescence of overexpressed Aes, Maml1, and Rbpj in HCT116 cells. Note colocalization of Aes, Maml1, and Rbpj in nuclear foci (arrowheads). Scale bar, 10 μm.

(F) Immunofluorescence of overexpressed RAMIC, Maml1 and Rbpj in HCT116 cells. Note colocalization of Maml1, RAMIC, and Rbpj in nuclear foci in the presence of Aes and TLE1 (arrowheads). Scale bars, 10 μm.

(G) Effects of Aes and TLE1 on localization of Maml1 and transcription activity in the nucleus. HCT116 cells were transfected with expression plasmids for TLE1, Maml1, RAMIC and simultaneously with or without AcGFP-Aes and TLE1. Twenty-four hours later, the transfectants were pulse-labeled with BrUTP. Anti-BrUTP antibody localized newly synthesized mRNA in the nucleus. Note that Aes and Maml1 colocalized in the nuclear foci where few BrUTP speckles were observed.

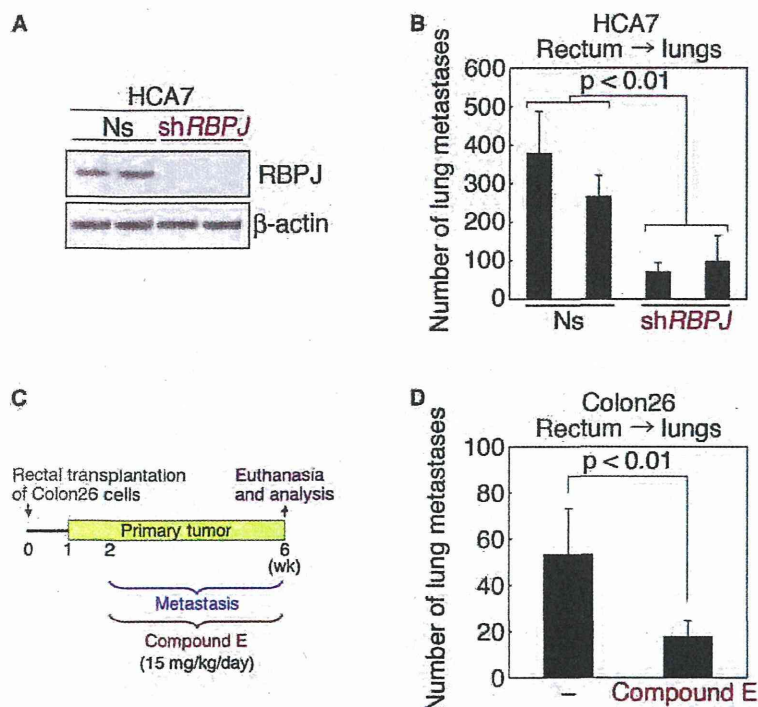


Figure 5. Suppression of Colon Cancer Metastasis by Inhibition of Notch Signaling

(A) Construction of HCA7 derivatives with constitutive expression of shRNA sequences against *RBPJ* mRNA (*shRBPJ*), confirmed by western blotting. Clones were isolated using two different shRNAs. β -Actin is shown as a loading control. Ns, nonsilencing controls.

(B) Effects of *shRBPJ* on lung metastasis of HCA7 derivatives transplanted into the nude mouse rectum. Error bars indicate SD ($n = 10$).

(C) Dosing scheme of Compound E for mice bearing Colon26 rectal tumors.

(D) Effects of Compound E on lung metastasis of Colon26 rectal tumors in Balb/c mice. —, Vehicle control. Data set shown is a representative of two. Error bars indicate SD ($n = 8$).

See also Figure S5.

called “adenocarcinomas” by histopathological definition, the extent of cellular atypia and epithelial architecture were rather similar to those in the *Apc* ^{Δ 716} adenomas, without a very malignant appearance.

As in the transplantation results above (Figures S6A–S6C), blood vessels and macrophages expressed Dll4 ligand also in the *Apc/Aes* tumors (Figures 7H–7K). In addition, we found that smooth muscle layers as well as *muscularis mucosae* also expressed Dll4 ligand, although the invading tumor epithelium scarcely did (Figures 7L and 7M). Notably, the expression level of tumor *Hes1* was 1.5 times higher in *Apc/Aes* compound mutants than in *Apc* mutants (Figure 7N). Furthermore, treatment of the *Apc/Aes* mice with Compound E inhibited the tumor invasion significantly (Figure 7O), indicating a key role of Notch signaling in the invasion that was caused by *Aes* knockout. On the other hand, knocking out *Aes* did not affect the tumor size or number. (Figure 7P).

DISCUSSION

In this study, we have demonstrated that *Aes* inhibits metastasis of colon cancer cells in an orthotopic transplantation model in

adenocarcinomas. The latter tumors were surrounded by immature myeloid cells (IMCs; CD34⁺CD45⁺CCR1⁺) and showed local invasion without intravasation (Kitamura et al., 2007; Kitamura and Taketo, 2007). In contrast, there were few IMCs around the invasion fronts of *Apc/Aes* tumors (data not shown), suggesting that tumors of these two models invade by different mechanisms.

Proliferation of Colon26 cells remained unaffected by *Aes* overexpression or knockdown, either in culture or upon grafting to the mouse rectum (Figures S2F–S2H; data not shown). Furthermore, the tumor number or size was not affected by the conditional *Aes* knockout (Figure 7P). Therefore, we conclude that *Aes* is an endogenous “metastasis suppressor” that inhibits metastasis but not tumorigenicity (Steeg, 2006; Smith and Theodorescu, 2009).

During the short life span of the *Apc/Aes* mutant mice (<18 weeks), we have been unable to find any overt metastasis in either liver or lungs. Because we initially used Colon26 cell line to find *Aes* gene downregulation in liver metastasis, we reasoned this difference from the *Apc/Aes* phenotype as below. First, the method of Colon26 injection into the rectal smooth muscle bypasses the local invasion, as well as intravasation

(arrowheads). On the other hand, in the absence of *Aes*, Maml1 distributed throughout the nucleoplasm where BrUTP was present (asterisks). Different from the top row photo, BrUTP-unstained area in AcGFP (bottom; marked as +) are also unstained for Maml1 in the left panel, suggesting that these areas are nucleoli rather than the foci. Scale bars, 10 μ m.

(H) Colocalization of *Aes* and *Rbpj* on the nuclear matrix. HCT116 cells were transfected with expression plasmids for AcGFP or AcGFP-*Aes* simultaneously with TLE1, *Rbpj*, *RAMIC*, and Maml1. Twenty-four hours later, localization of the overexpressed proteins was analyzed by immunofluorescence (arrowheads in Whole cell). Note that AcGFP-*Aes* and *Rbpj* were retained inside the cells even after soluble proteins were washed off (arrowheads in Nuclear matrix). In contrast, *Rbpj* did not remain in the cells in the absence of *Aes*. Scale bars, 10 μ m.

See also Figure S4.

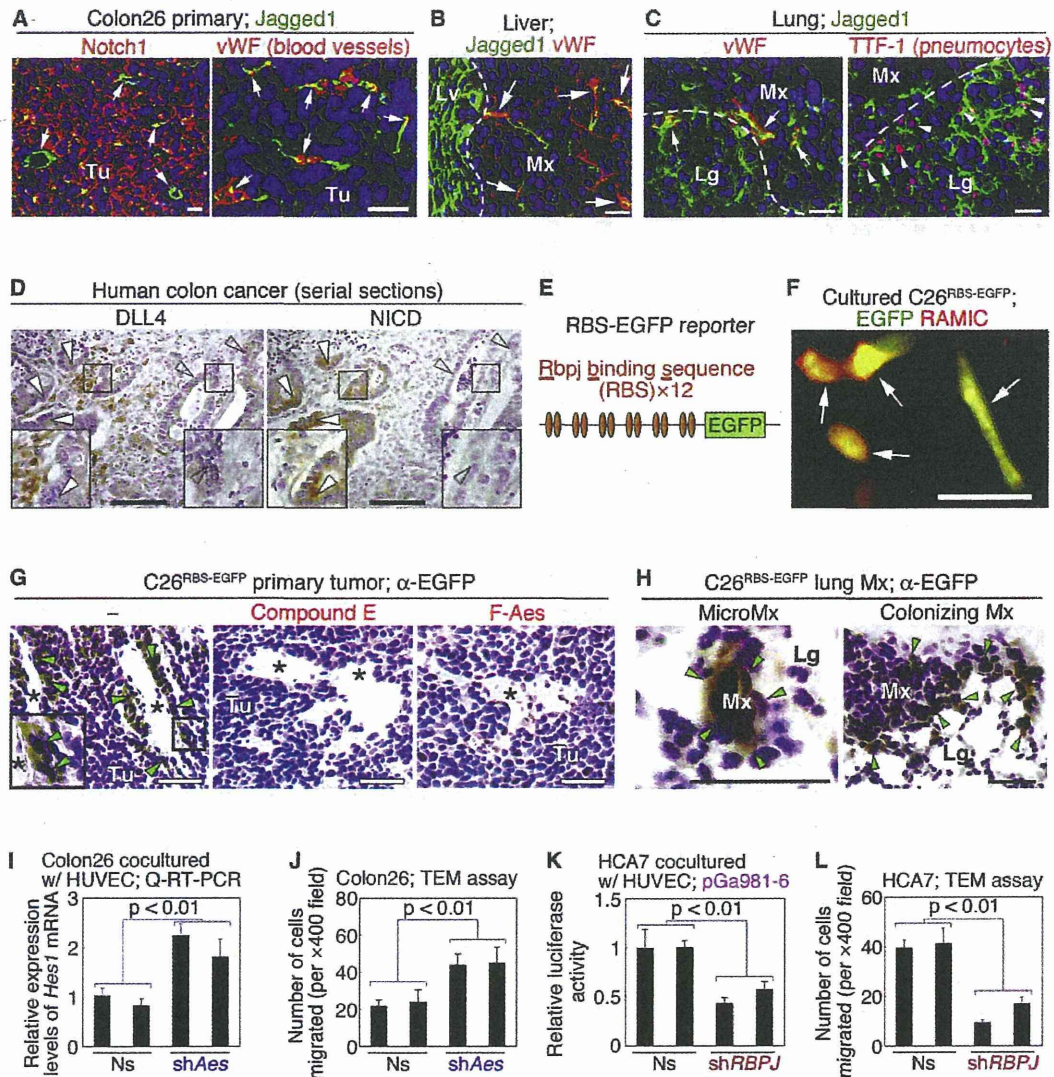


Figure 6. Activation of Notch Signaling in Cancer Cells by Adjoining Blood Endothelial Cells and Macrophages

(A) Immunofluorescence staining of Jagged1 (green) in a Colon26 tumor of the rectum. Red staining shows Notch1 (left) or blood vessel marker vWF (von Willebrand factor; right). DNA was stained with DAPI (blue). Arrows point representative Jagged1-expressing blood vessels. Tu, Tumor. Scale bars, 10 μ m. (B and C) Immunofluorescence staining of Jagged1 (green) in the liver (B) and lung (C) with Colon26 metastases. Red staining shows vWF, or thyroid transcription factor (TTF) -1, a pneumocyte marker (C; right). Arrows and arrowheads point to the representative Jagged1-expressing blood vessels and pneumocytes adjoining the metastatic foci, respectively. Broken lines indicate the boundaries between the metastases and liver or lung tissues. Mx, metastasis. Lv and Lg, normal liver and lung tissues, respectively. DNA was stained with DAPI (blue). Scale bars, 10 μ m. (D) Close proximity of DLL4-expressing cells with NICD-expressing cells in human colon cancer. Serial sections were immunostained with anti-DLL4 (left) and anti-NICD (right) antibodies, respectively. Note that DLL4 was expressed in the stroma close to the cancer epithelium where NICD was stained (closed arrowheads in left insets). In contrast, cancer epithelium surrounded by DLL4-negative stroma showed little NICD staining (open arrowheads in right insets). Bars, 100 μ m. (E) A schematic representation of the RBS-EGFP reporter construct. The Notch signaling causes expression of EGFP through the tandem repeats of Rbpj binding sequence (RBS). The reporter was introduced into Colon26 cells to derive C26^{RBS-EGFP} cells. (F) Induction of EGFP in response to RAMIC expression in C26^{RBS-EGFP} cells. An expression vector for myc-tagged RAMIC was transfected into the C26^{RBS-EGFP} cells. Autofluorescence of EGFP and immunofluorescence signal of myc (red) were photographed under a fluorescence microscope, and merged electronically. Note that EGFP was induced in most of the RAMIC-expressing cells, merging as yellow (arrows). Scale bar, 10 μ m. (G and H) Activation of the Notch signaling within Colon26 primary tumors of the rectum (G, left) and its metastasis to the lung (H), detected by immunostaining for EGFP (green arrowheads). Boxed area in the left panel of (G) is enlarged in the inset. Note that treatment with Compound E (G, center) or overexpression of flag-tagged Aes (G, right) suppressed induction of EGFP. Asterisks, blood vessel lumens. Tu, tumor. Mx, metastasis. Lg, normal lung tissue. Scale bars, 50 μ m.

because some fine vessels are destroyed upon injection. Second, Colon26 cells contain an activated *Kras* mutation allele. Accordingly, additional mutations in the *Apc/Aes* mutant mice may lead to overt metastasis of the intestinal tumors to distant organs.

Curiously, some of the cancer cells had already lost expression of *AES/Aes* on the invasion fronts in both human (Figure 1D, inset in the left panel) and mouse (Figure 1E) colon primary tumors. These results suggest that expression of *AES/Aes* is downregulated during the expansion of primary tumors. When cancer cells lose *Aes*, they can acquire the capacity to invade and intravasate. The mechanisms by which expression of *Aes* is downregulated remain to be investigated. We searched for *AES* mutations in colon cancer cell lines, without evidence so far. Although we tested the possibility of DNA methylation by treating colon cancer cell lines that lack *AES* with 5-aza-2-deoxycytidine, we found no increases in its expression. Thus, we speculate that *AES/Aes* gene is inactivated through some epigenetic changes other than DNA methylation.

Interestingly, we found that *Aes* colocalized with TLE1, Rbpj, RAMIC and Maml1 in nuclear foci where transcription is repressed (Figures 4D–4H). Because *Aes* is also associated and colocalized with HDAC3 in the foci (Figure S4), we speculate that *Aes* converts the transactivation complex to the MAD (matrix-associated deacetylase) bodies where HDAC proteins repress the Rbpj-dependent transcription (Kao et al., 1998; Downes et al., 2000). These results are consistent with reports that Notch repressors including SMRT and Mint/Sharp/Spen also show a similar speckled pattern in the nucleus (Kao et al., 1998; Downes et al., 2000; Oswald et al., 2002; Shi et al., 2001). Curiously, *Aes* null mice show a dwarf phenotype (Mallo et al., 1995, and data not shown). The dwarfism is caused by reduction in growth hormone-producing cells in the pituitary (Brinkmeier et al., 2003). Notably, the same dwarf phenotype is also reported in the transgenic mice overexpressing NICD, and in conditional knockout mice of the *Mint* gene (Zhu et al., 2006; Yabe et al., 2007), supporting the Notch-suppressing role of *Aes* in vivo.

It is possible that the elementary processes stimulated by Notch signaling are the motility and migration as implicated by our initial analysis of *Aes* in Matrigel (Figure S1G) and simpler scratch assays using recombinant Notch ligands (Figure S6F). Thus, we speculate that the enhanced motility contributes to TEM activity of cancer cells. It is conceivable that Notch signaling affects, either directly or indirectly, a series of small G proteins of the Rho family that can control the assembly of the actin cytoskeleton, as cell motility is regulated by such molecules (Weinberg, 2007). While these steps may be achieved by

some carcinoma cells through a program of epithelial-mesenchymal transition (EMT), we have been unable to find signs of EMT in the Notch signaling-activated colon cancer or intestinal tumor cells. For example, tumor cells in the *Apc/Aes* compound mutants retained expression of cytokeratins and E-cadherin (Figures 7G–7I; data not shown) whose loss is a hallmark of EMT (Weinberg, 2007). Furthermore, expression of *Snail*, *Slug*, or *Twist* in Colon26 cells did not change upon transfection of *Aes* (data not shown). So far, about ten metastasis suppressor genes have been reported (Steege, 2006; Smith and Theodorescu, 2009). Many of them appear to be involved in later steps in the metastasis cascade such as colonization, whereas some are involved in signal transduction pathways, including MAP kinase, Rho, Rac, and G protein-coupled and tyrosine kinase receptors. The effects of *Aes* downregulation in mutant mice on these genes remain to be investigated.

We found that Notch ligands Jagged1 and Dll4 were present on endothelial cells of the liver and lungs. Furthermore, we found ligand expression also on normal epithelium of the metastasis target organs (Figures 6B and 6C; Figures S6B and S6C). Convincingly, we found activated Notch signaling (expression of EGFP as a readout) in two types of metastasized cell clusters in the lung; micrometastases consisting of only a few cancer cells, and cells at the periphery of larger metastases that were expanding in the lung parenchyma (Figure 6H). Considering the fact that *Aes* can inhibit metastasis of cancer cells injected intravenously, we speculate that *Aes* also attenuates extravasation at the target organs. In addition, the ligand-expressing parenchymal cells adjoining the cancer cells may facilitate the metastatic expansion through stimulation of cancer invasion into the surrounding tissues, and inhibition of apoptosis in cancer cells (Artavanis-Tsakonas et al., 1999).

By searching the ONCOMINE database (<http://www.oncomine.org/>), we found that data were compiled showing the correlation between *AES* downregulation and metastasis for a variety of cancers such as prostate, bladder, breast, and ovarian cancers, and sarcoma, neuroblastoma, etc. These data suggest that *AES* has a metastasis-suppressing role also in other types of cancer. Furthermore, these results imply that earlier steps of the invasion-metastasis cascade are probably similar in various types of human tumors, although the last step—colonization—is likely to depend on complex interactions between the metastasizing cells and microenvironments of the host tissues where they land (Weinberg, 2007).

In summary, we have demonstrated that *Aes* is a metastasis suppressor that prevents local tumor invasion and intravasation through inhibition of Notch signaling. When cancer cells retain expression of *Aes*, it suppresses Notch signaling that is triggered

(I) Effects of *Aes* knockdown by shRNA against *Aes* mRNA (sh*Aes*) on Notch signaling. Colon26 cells with (sh*Aes*) or without (Ns; nonsilencing) constitutive expression of sh*Aes* were cocultured with HUVEC. Twelve hours later, cells were harvested and expression of mouse *Hes1* mRNA was quantified. Error bars indicate SD (n = 3).

(J) Effects of sh*Aes* on transendothelial migration (TEM) of Colon26 cells. Twenty-four hours after coculture, Colon26 cells that had migrated through the HUVEC layer were counted. Error bars indicate SD (n = 3).

(K) Effects of shRNA against *RBPJ* mRNA (sh*RBPJ*) on Notch signaling. Two independent HCA7 clones were derived by introducing nonsilencing control (Ns) and *RBPJ* knockdown (sh*RBPJ*) constructs, respectively, and transfected with the luciferase reporter followed by coculture with HUVEC. At 12 hr posttransfection, luciferase activity was determined. Error bars indicate SD (n = 3).

(L) Effects of sh*RBPJ* on TEM activity of HCA7 cancer cells. HCA7 cells were placed on a layer of HUVEC. Twenty-four hours later, HCA7 cells were counted that had migrated through the HUVEC layer. Error bars in (I–L) indicate SD of three independent experiments.

See also Figure S6 and Movie S1.

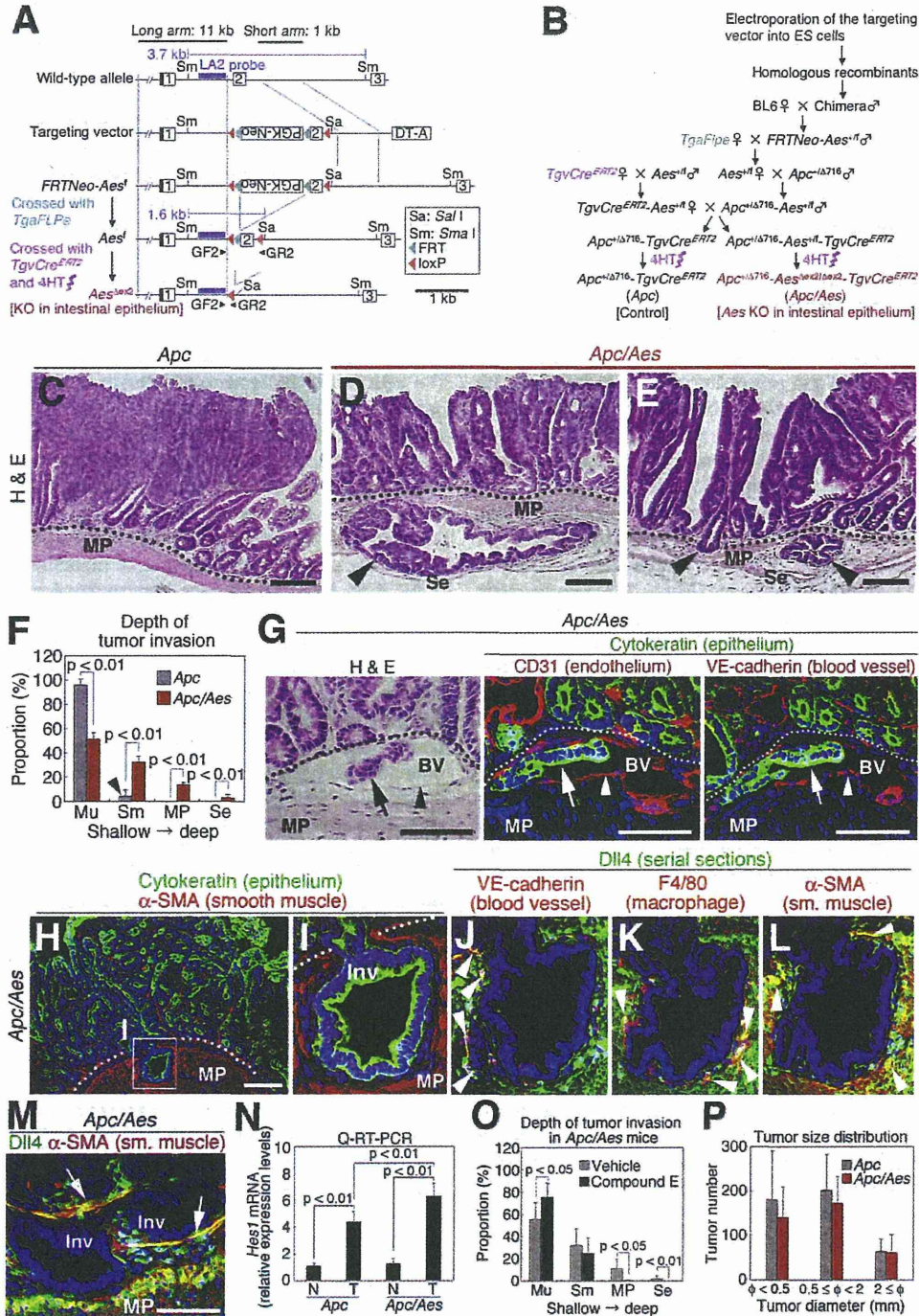


Figure 7. Local Tumor Invasion and Intravasation Phenotypes of the Compound Knockout Mice for *Aes* and *Apc* Genes

(A) Targeting strategy for the *Aes* allele specifically in the intestinal epithelium. Restriction sites and a Southern blotting probe are shown. PCR primers GF2 and GR2 were used to distinguish the floxed allele (*Aes^{fl}*) from the targeted allele (*Aes^{ox2}*) of *Aes* gene after Cre activation by 4-hydroxytamoxifen (4HT). (B) Breeding scheme for generating *Apc^{Δ716}-Aes^{fl}-TgvlCre^{ERT2}* compound mutants. Germline mice with the targeted *Aes* allele flanked by a PGK-Neo cassette (*FRTNeo-Aes^{fl}*) were crossed with a transgenic strain where expression of Fipe was driven by actin promoter (*TgvlFipe*) to remove the cassette. Resulting *Aes^{fl}* mice were crossed with another transgenic strain carrying an expression cassette for Cre^{ERT2} driven by villin promoter (*TgvlCre^{ERT2}*) and *Apc* knockout mice (*Apc^{Δ716}*), to generate *Apc^{Δ716}-Aes^{fl}-TgvlCre^{ERT2}* compound mutant mice. Treating them with 4HT activated Cre^{ERT2}, knocking out the *Aes* gene (*Apc/Aes*).

Cancer Cell

Metastasis Suppressor Aes Inhibits Notch Signaling

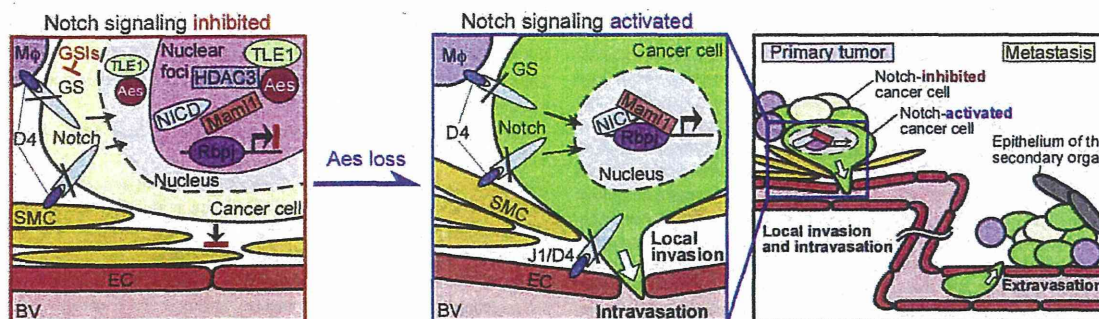


Figure 8. A Schematic Representation of Aes as a Notch Signaling Inhibitor, Hence a Metastasis Suppressor

When Notch receptor on a cancer cell is bound by Dll4 (D4) or Jagged1 (J1) ligand on adjoining macrophages (M ϕ), smooth muscle cells (SMC), or endothelial cells (EC), Notch intracellular domain (NICD) is released by γ -secretase (GS) cleavage. We propose that Aes relocates to nuclear foci with TLE1, Rbpj, NICD, Maml1, and HDAC3, to repress transcription (left). Once Aes is lost in a cancer cell, the transcription is derepressed, stimulating its local invasion and intravasation into the blood vessel (BV, center). In addition, Notch signaling is likely to promote extravasation of the cancer cell at the target organ, enhancing its metastasis (right). GSIs, GS inhibitors.

by the stromal cells (Figure 8, left). Once cancer cells lose its expression, derepressed Notch signaling can stimulate their local invasion (Figure 8, center), enhancing intravasation to promote metastasis (Figure 8, right). Because numerous compounds and biologicals have been evaluated as Notch signaling inhibitors, it is possible that some of such agents prove clinically efficacious in the treatment and prevention of cancer metastasis.

EXPERIMENTAL PROCEDURES

Animals

Balb/c, C57BL/6, and nude mice were purchased from CLEA (Japan). *Apc* ^{Δ 716} and *TgvCre*^{ERT2} mice have been described previously (Oshima et al., 1995; el Marjou et al., 2004). *TgaFlpe* mice were obtained from the Jackson Laboratory. All animal experiments were conducted according to the protocol approved by the Animal Care and Use Committee of Kyoto University.

Microarray Analysis

RNA samples were prepared from Colon26 cells in primary tumors and their liver metastases using TRI reagent (SIGMA). Gene expression profiles were analyzed using 3D-Gene Mouse Oligo Chip 24k (TORAY).

Clinical Samples

Cancer tissues had been resected from patients who had undergone operations with informed consents, with the protocol approved by the Ethics Committee of Kyoto University or Kitano Hospital. Tumors were fixed by formalin and embedded in paraffin wax.

Conditional Knockout of Aes Allele

As shown in Figure 7A, we constructed a targeting vector where the PGK-Neo cassette sandwiched with FRT sequences was inserted into intron 1 immediately 5' to exon 2 of *Aes*, followed by addition of loxP sequences sandwiching the insert and exon 2. The vector was constructed using the recombinering technology (Liu et al., 2003). A BAC clone bMQ-222K13 containing whole *Aes* gene of 129 strain was obtained from Geneservice (UK). A 13 kb DNA fragment spanning from 8 kb upstream of exon 1 to 2 kb downstream of exon 2 was retrieved from the BAC, and subcloned into pMCS-DTA vector to construct "pMCS-DTA-Aes" using SW102 strain of *Escherichia coli*. A PGK-Neo cassette sandwiched with two loxP sequences was excised from PL452 plasmid and inserted at downstream of exon 2 in pMCS-DTA-Aes to construct "pMCS-DTA-loxNeo-Aes." After induction of Cre recombinase by arabinose in SW106 strain of *E.coli*, the pMCS-DTA-loxNeo-Aes was introduced into the SW106. Upon Cre-mediated excision of the PGK-Neo cassette, one loxP sequence was left at downstream of exon 2, creating "pMCS-DTA-lox-Aes." Then a PGK-Neo cassette sandwiched with two FRT

(C–E) Histopathology of the small intestine at 17 weeks of age (H & E). In the control (*Apc*), adenoma cells remained above the *muscularis mucosae* (dotted line; C). In the *Apc/Aes* compound mutant mice, tumor cells invaded the *muscularis mucosae* and *muscularis propria* (MP), reaching the *serosa* (Se) (arrowheads in D and E). Scale bars, 100 μ m.

(F) Quantification of the depth of tumor invasion in the small intestine at 17 weeks of age. Note that the tumor cells in the compound mutants (*Apc/Aes*; red) but not controls (*Apc*; gray) deeply invaded into the *submucosa* (Sm). Mu, *mucosa*. MP, *muscularis propria*. Se, *serosa*. Arrowhead, pseudoinvasion (herniation) in *Apc* control. n = 5 for each group.

(G) Tumor intravasation in the *Apc/Aes* mice. Left, An H&E staining suggested tumor cells (arrow) inside a blood vessel (BV; also indicated by arrowhead) near the *muscularis mucosae* (dotted line). This interpretation was verified by immunofluorescence in the adjoining sections for epithelial marker cytokeratin (green; arrow), and vessel marker CD31 (red; center) as well as blood vessel marker VE-cadherin (right). MP, *muscularis propria*. Scale bars, 50 μ m.

(H–L) Expression of Dll4 ligand on stromal cells analyzed by immunostaining of serial sections. Epithelial cells express cytokeratin (green), whereas smooth muscle cells (MP; *muscularis propria*) express α -smooth muscle actin (α -SMA in red; H). Boxed area in (H) is enlarged in (I), whose serial sections are (J), (K), and (L). Blood vessels (stained for VE-cadherin in red; J), macrophages (F4/80 in red; K), and smooth muscle (α -SMA in red; L) expressed Dll4 (green) merging as yellow (arrowheads) around the local invasion of tumor epithelium. Scale bar, 100 μ m.

(M) Immunofluorescence of Dll4 (green) and α -SMA (red) in the invading tumor of the *Apc/Aes* mutant (Inv). Note that smooth muscle cells in the *muscularis mucosae* (arrows) as well as the *muscularis propria* (MP) expressed Dll4 ligand. Scale bar, 50 μ m.

(N) Expression levels of *Hes1* mRNA in the mouse small intestine determined by Q-RT-PCR. N, normal mucosa. T, tumor. Error bars indicate SD (n = 5).

(O) Effects of Compound E on depth of tumor invasion. *Apc/Aes* mice were treated with (black bars) or without (gray bars) Compound E for 10 weeks. Error bars indicate SD (n = 5 for each group).

(P) Size distribution of tumors in the small intestine at 17 weeks of age. Control *Apc* is shown in gray, whereas *Apc/Aes* is indicated in red. Error bars indicate SD (n = 5).

See also Figure S7.

sequences followed by a loxP sequence was excised from PL451 plasmid (NCI), and inserted upstream of exon 2, generating the targeting vector "pMCS-DTA-FRTNeo-Aes^{fl}" (Figure 7A). The integrity of the construct was verified by PCR and restriction digestion after introduction of the vector into Cre-expressing SW106 or Flpe-expressing SW105 strains (NCI). Then, the vector was introduced into D3a2 ES cells by homologous recombination and targeted ES clones were selected and karyotyped. Germ line-transmitted mice (FRTNeo-Aes^{+/fl}) were generated and the PGK-Neo selection sequence was removed by crossing with actin promoter-driven FLPe transgenic mice (TgaFlpe) (Jackson Laboratory, ME), producing mice with a floxed Aes allele (Aes^{+/fl}) (Figure S7B). We verified that homozygotes of these floxed Aes wild-types are viable, fertile and without any obvious phenotypes (data not shown). As shown in Figure 7B, we then crossed these Aes^{+/fl} female mice with Apc^{+/Δ716} males, and further crossed their compound heterozygotes with the compound heterozygotes obtained from crosses between Aes^{+/fl} males and Villin-Cre^{ERT2} transgenic (TgvCre^{ERT2}) females. At 3 weeks of age, the progeny compound mutant mice (Apc^{+/Δ716}-Aes^{fl/fl}-TgvCre^{ERT2}) were treated with 4-hydroxytamoxifen (4HT; SIGMA) to activate Cre recombinase in the intestine-specific manner (el Marjou et al., 2004), generating Apc^{+/Δ716}-Aes^{Δex2/Δex2}-TgvCre^{ERT2}, abbreviated as Apc/Aes.

Data Analysis

Data were analyzed by Student's t or chi-square tests and are presented as mean ± SD. P values <0.05 were considered significant.

ACCESSION NUMBERS

Microarray hybridization data have been deposited in the GEO database with accession code GSE12162.

SUPPLEMENTAL INFORMATION

Supplemental Information includes Supplemental Experimental Procedures, seven figures, and two movies and can be found with this article online at doi:10.1016/j.ccr.2010.11.008.

ACKNOWLEDGMENTS

We thank H. Kikuchi and Y. Mouri for excellent technical assistance, T. Honjo for plasmids and suggestions, T. Sudo for microarray analyses, Y. Yui and T. Tanaka for time-lapse microphotography, O. Takahashi for high-magnification fluorescence microphotography, S. Stifani for anti-pantTLE antibody, H. Sasaki for Hedgehog reporters, T. Ishikawa, H. Miyoshi, A. Deguchi, S. Arimura, S. Yamashita, I. Okazaki, T. Okazaki, K. Okawa, C. Takahashi, T. Tomita, and Y. Morohashi for helpful discussions, S. Takahashi for microinjection of ES cells into blastocysts, N. Copeland, N. Jenkins, J. Takeda, and K. Yusa for biologicals and suggestions for the recombineering system. We also thank P. Vogt, To. Kitamura, M. Okabe, M. Kitagawa, and S. Kirkland for providing vectors pBSf1-AU1-TLE1, pMX-IRES-EGFP, pCX, Mami1 cDNA and HCA7 cells, respectively. This work was supported by grants from Ministry of Education, Culture, Sports, Science and Technology (MEXT), Japan, and by Jeannik M. Littlefield-AACR Grant in Metastatic Colon Cancer Research.

Received: June 7, 2010

Revised: September 17, 2010

Accepted: November 2, 2010

Published: January 18, 2011

REFERENCES

Artavanis-Tsakonas, S., Rand, M.D., and Lake, R.J. (1999). Notch signaling: cell fate control and signal integration in development. *Science* **284**, 770–776.
 Brantjes, H., Roose, J., van de Wetering, M., and Clevers, H. (2001). All Tcf HMG box transcription factors interact with Groucho-related co-repressors. *Nucleic Acids Res.* **29**, 1410–1419.

Brinkmeier, M.L., Potok, M.A., Cha, K.B., Gridley, T., Stifani, S., Meeldijk, J., Clevers, H., and Camber, S.A. (2003). TCF and Groucho-related genes influence pituitary growth and development. *Mol. Endocrinol.* **17**, 2152–2161.
 Chen, G., and Courey, A.J. (2000). Groucho/TLE family proteins and transcriptional repression. *Gene* **249**, 1–16.

Christoforo, G. (2006). New signals from the invasive front. *Nature* **441**, 444–450.

Corbett, T.H., Griswold, D.P., Jr., Roberts, B.J., Peckham, J.C., and Schabel, F.M., Jr. (1975). Tumor induction relationships in development of transplantable cancers of the colon in mice for chemotherapy assays, with a note on carcinogen structure. *Cancer Res.* **35**, 2434–2439.

Detre, S., Saclani Jotti, G., and Dowsett, M. (1995). A "quickscore" method for immunohistochemical semiquantitation: validation for oestrogen receptor in breast carcinomas. *J. Clin. Pathol.* **48**, 876–878.

Downes, M., Ordentlich, P., Kao, H.-Y., Alvarez, J.G.A., and Evans, R.M. (2000). Identification of a nuclear domain with deacetylase activity. *Proc. Natl. Acad. Sci. USA* **97**, 10330–10335.

el Marjou, F., Janssen, K.P., Chang, B.H., Li, M., Hindie, V., Chan, L., Louvard, D., Chambon, P., Metzger, D., and Robine, S. (2004). Tissue-specific and inducible Cre-mediated recombination in the gut epithelium. *Genesis* **39**, 186–193.

Fidler, I.J. (2003). The pathogenesis of cancer metastasis: the "seed and soil" hypothesis revisited. *Nat. Rev. Cancer* **3**, 453–458.

Gasperowicz, M., and Otto, F. (2005). Mammalian Groucho homologs: redundancy or specificity? *J. Cell. Biochem.* **95**, 670–687.

Hoshino, H., Nishino, T.G., Tashiro, S., Miyazaki, M., Ohmiya, Y., Igarashi, K., Horinouchi, S., and Yoshida, M. (2007). Co-repressor SMRT and class II histone deacetylase promote Bach2 nuclear retention and formation of nuclear foci that are responsible for local transcriptional repression. *J. Biochem.* **141**, 719–727.

Hurlbut, G.D., Kankel, M.W., Lake, R.J., and Artavanis-Tsakonas, S. (2007). Crossing paths with Notch in the hyper-network. *Curr. Opin. Cell Biol.* **19**, 166–175.

Ilagan, M.X., and Kopan, R. (2007). Snapshot: Notch signaling pathway. *Cell* **128**, 1246.

Kao, H.-Y., Ordentlich, P., Koyano-Nakagawa, N., Tang, Z., Downes, M., Kintner, C.R., Evans, R.M., and Kadesch, T. (1998). A histone deacetylase corepressor complex regulates the Notch signal transduction pathway. *Genes Dev.* **12**, 2269–2277.

Kashtan, H., Rabau, M., Mullen, J.B.M., Wong, A.H.C., Roder, J.C., Shpitz, B., Stern, H.S., and Gallinger, S. (1992). Intra-rectal injection of tumor cells: a novel animal model of rectal cancer. *Surg. Oncol.* **1**, 251–256.

Kato, H., Taniguchi, Y., Kurooka, H., Minoguchi, S., Sakai, T., Nomura-Okazaki, S., Tamura, K., and Honjo, T. (1997). Involvement of RBP-J in biological functions of mouse Notch1 and its derivatives. *Development* **124**, 4133–4141.

Kirkland, S.C. (1985). Dome formation by human colonic adenocarcinoma cell line (HCA-7). *Cancer Res.* **45**, 3790–3795.

Kitamura, T., and Taketo, M.M. (2007). Keeping out the bad guys: gateway to cellular target therapy. *Cancer Res.* **67**, 10099–10102.

Kitamura, T., Kometani, K., Hashida, H., Matsunaga, A., Miyoshi, H., Hosogi, H., Aoki, M., Oshima, M., Hattori, M., Takabayashi, A., et al. (2007). SMAD4-deficient intestinal tumors recruit CCR1⁺ myeloid cells that promote invasion. *Nat. Genet.* **39**, 467–475.

Lepourcelet, M., and Shivdasani, R.A. (2002). Characterization of a novel mammalian Groucho isoform and its role in transcriptional regulation. *J. Biol. Chem.* **277**, 47732–47740.

Liu, P., Jenkins, N.A., and Copeland, N.G. (2003). A highly efficient recombineering-based method for generating conditional knockout mutations. *Genome Res.* **13**, 476–484.

Lu, C., Bonome, T., Li, Y., Kmat, A.A., Han, L.Y., Schmandt, R., Coleman, R.L., Gershenson, D.M., Jaffe, R.B., Birrer, M.J., et al. (2007). Gene alterations identified by expression profiling in tumor-associated endothelial cells from invasive ovarian carcinoma. *Cancer Res.* **67**, 1757–1768.

- Mailhos, C., Modlich, U., Lewis, J., Harris, A., Bicknell, R., and Ish-Horowitz, D. (2001). Delta4, an endothelial specific notch ligand expressed at sites of physiological and tumor angiogenesis. *Differentiation* 69, 135–144.
- Mallo, M., Gendron-Maguire, M., Harbison, M.L., and Gridley, T. (1995). Protein characterization and targeted disruption of *Grg*, a mouse gene related to the *groucho* transcript of the *Drosophila Enhancer of split* complex. *Dev. Dyn.* 204, 338–347.
- Milano, J., McKay, J., Dagenais, C., Foster-Brown, L., Pognan, F., Gadiant, R., Jacobs, R.T., Zacco, A., Greenberg, B., and Ciaccio, P.J. (2004). Modulation of Notch processing by γ -secretase inhibitors causes intestinal goblet cell metaplasia and induction of genes known to specify gut secretory lineage differentiation. *Toxicol. Sci.* 82, 341–358.
- Oshima, M., Oshima, H., Kitagawa, K., Kobayashi, M., Itakura, C., and Taketo, M. (1995). Loss of *Apc* heterozygosity and abnormal tissue building in nascent intestinal polyps in mice carrying a truncated *Apc* gene. *Proc. Natl. Acad. Sci. USA* 92, 4482–4486.
- Oswald, F., Kostezka, U., Astrahantseff, K., Bourteele, S., Dillinger, K., Zechner, U., Ludwig, L., Wilda, M., Hameister, H., Knöchel, W., et al. (2002). SHARP is a novel component of the Notch/RBP-J κ signalling pathway. *EMBO J.* 21, 5417–5426.
- Pinto, M., and Lobe, C.G. (1996). Products of the *grg* (*Groucho-related gene*) family can dimerize through the amino-terminal Q domain. *J. Biol. Chem.* 271, 33026–33031.
- Price, J.E. (2001). Xenograft models in immunodeficient animals: I. nude mice. In *Methods in molecular medicine: Metastasis research protocols, Volume II*, S.A. Brooks and U. Schumacher, eds. (Totowa, NJ: Humana Press), pp. 205–214.
- Roose, J., Molenaar, M., Peterson, J., Kurenkamp, J., Brantjes, H., Moerer, P., van de Wetering, M., Destree, O., and Clevers, H. (1998). The *Xenopus* Wnt effector XTcf-3 interacts with Groucho-related transcriptional repressors. *Nature* 395, 608–612.
- Sancho, E., Battle, E., and Clevers, H. (2004). Signaling pathways in intestinal development and cancer. *Annu. Rev. Cell Dev. Biol.* 20, 695–723.
- Schmidt, B. (2003). Aspartic proteases involved in Alzheimer's disease. *ChemBioChem* 4, 366–378.
- Shi, Y., Downes, M., Xie, W., Kao, H.Y., Ordentlich, P., Tsai, C.C., Hon, M., and Evans, R.M. (2001). Sharp, an inducible cofactor that integrates nuclear receptor repression and activation. *Genes Dev.* 15, 1140–1151.
- Smith, S.C., and Theodorescu, D. (2009). Learning therapeutic lessons from metastasis suppressor proteins. *Nat. Rev. Cancer* 9, 253–264.
- Steeg, P.S. (2006). Tumor metastasis: mechanistic insights and clinical challenges. *Nat. Med.* 12, 895–904.
- Takaku, K., Oshima, M., Miyoshi, H., Matsui, M., Seldin, M.F., and Taketo, M.M. (1998). Intestinal tumorigenesis in compound mutant mice of both *Dpc4* (*Smad4*) and *Apc* genes. *Cell* 92, 645–656.
- Taketo, M.M. (2006). Wnt signaling and gastrointestinal tumorigenesis in mouse models. *Oncogene* 25, 7522–7530.
- Taketo, M.M., and Edelman, W. (2009). Mouse models of colon cancer. *Gastroenterology* 136, 780–798.
- Tsutsumi, S., Kuwano, H., Morinaga, N., Shimura, T., and Asao, T. (2001). Animal model of para-aortic lymph node metastasis. *Cancer Lett.* 169, 77–85.
- van Es, J.H., Jay, P., Gregorieff, A., van Gijn, M.E., Jonkhoeer, S., Hatzis, P., Thiel, T.J., van den Born, M., Begthel, H., Brabletz, T., et al. (2005). Wnt signaling induces maturation of Paneth cells in intestinal crypts. *Nat. Cell Biol.* 7, 381–386.
- Wang, W.F., Wang, Y.G., Reginato, A.M., Plotkina, S., Gridley, T., and Olsen, B.R. (2002). Growth defect in *Grg5* null mice is associated with reduced Ihh signaling in growth plates. *Dev. Dyn.* 224, 79–89.
- Weinberg, R.A. (2007). Moving out: invasion and metastasis. In *The Biology of Cancer* (New York: Garland Science), pp. 587–654.
- Yabe, D., Fukuda, H., Aoki, M., Yamada, S., Takebayashi, S., Shinkura, R., Yamamoto, N., and Honjo, T. (2007). Generation of a conditional knockout allele for mammalian Spen protein Mint/SHARP. *Genesis* 45, 300–306.
- Zaczek, R., Olson, R.E., Seiffert, D.A., and Thompson, L.A. (1999). Compounds for inhibiting beta-amyloid peptide release and/or its synthesis. *PCT Int. Appl. WO99/67221*.
- Zagouras, P., Stifani, S., Blaumueller, C.M., Carcangiu, M.L., and Artavanis-Tsakonas, S. (1995). Alterations in Notch signaling in neoplastic lesions of the human cervix. *Proc. Natl. Acad. Sci. USA* 92, 6414–6418.
- Zhu, X., Zhang, J., Tollkuhn, J., Ohsawa, R., Bresnick, E.H., Guillemot, F., Kagayama, R., and Rosenfeld, M. (2006). Sustained Notch signaling in progenitors is required for sequential emergence of distinct cell lineages during organogenesis. *Genes Dev.* 20, 2739–2753.
- Zimber, A., Nguyen, Q.D., and Gespach, C. (2004). Nuclear bodies and compartments: functional roles and cellular signaling in health and disease. *Cell. Signal.* 16, 1085–1104.

LKB1 Suppresses p21-activated Kinase-1 (PAK1) by Phosphorylation of Thr¹⁰⁹ in the p21-binding Domain^{*[5]}

Received for publication, October 25, 2009, and in revised form, March 22, 2010. Published, JBC Papers in Press, April 16, 2010, DOI 10.1074/jbc.M109.079137

Atsuko Deguchi[‡], Hiroyuki Miyoshi[‡], Yasushi Kojima[‡], Katsuya Okawa[§], Masahiro Aoki[‡], and Makoto M. Taketo^{*[5]}

From the [‡]Department of Pharmacology, Graduate School of Medicine, Kyoto University, Kyoto 606-8501, Japan and

[§]Drug Discovery Research Laboratories, Kyowa Hakko Kirin Co., Ltd., Shizuoka 411-8731, Japan

The serine/threonine protein kinase *LKB1* is a tumor suppressor gene mutated in Peutz-Jeghers syndrome patients. The mutations are found also in several types of sporadic cancer. Although *LKB1* is implicated in suppression of cell growth and metastasis, the detailed mechanisms have not yet been elucidated. In this study, we investigated the effect of *LKB1* on cell motility, whose acquisition occurs in early metastasis. The knock-down of *LKB1* enhanced cell migration and PAK1 activity in human colon cancer HCT116 cells, whereas forced expression of *LKB1* in *Lkb1*-null mouse embryonic fibroblasts suppressed PAK1 activity and PAK1-mediated cell migration simultaneously. Notably, *LKB1* directly phosphorylated PAK1 at Thr¹⁰⁹ in the p21-binding domain *in vitro*. The phosphomimetic T109E mutant showed significantly lower protein kinase activity than wild-type PAK1, suggesting that the phosphorylation at Thr¹⁰⁹ by *LKB1* was responsible for suppression of PAK1. Consistently, the nonphosphorylatable T109A mutant was resistant to suppression by *LKB1*. Furthermore, we found that PAK1 was activated in the hepatocellular carcinomas and the precancerous liver lesions of *Lkb1*(+/-) mice. Taken together, these results suggest that PAK1 is a direct downstream target of *LKB1* and plays an essential role in *LKB1*-induced suppression of cell migration.

LKB1 is a serine/threonine kinase whose mutations have been found not only in Peutz-Jeghers syndrome patients (1–3) but also in various types of sporadic cancer (4–6). These results suggest that *LKB1* is a tumor suppressor gene. In addition, we and others (7–9) have previously shown that the heterozygous *Lkb1* mutations in mice cause gastrointestinal hamartomas after 20 weeks of age and cause hepatocellular carcinomas (HCCs)² after 50 weeks (10). Notably, the *Lkb1* gene in all HCC

and hepatic precancerous lesions shows loss of heterozygosity (10, 11). These phenotypes in *Lkb1*(+/-) mice further indicate that *LKB1* is a tumor suppressor gene.

In mammalian cells, *LKB1* forms a complex with STE20-related adaptor pseudokinase (STRAD) and scaffolding protein MO25, both of which are required for *LKB1* enzymatic activity (12, 13). It can phosphorylate and activate at least 14 kinases, including AMP-activated protein kinase (AMPK) and microtubule-associated protein/microtubule affinity-regulating kinases (MARKs) (5). Activation of AMPK by *LKB1* leads to inactivation of mammalian target of rapamycin complex 1 via phosphorylation of the tuberous sclerosis complex 1/2, and this pathway has been implicated in tumor suppressor functions of *LKB1*. In addition to growth control, *LKB1* also plays important roles in establishing cell polarity in mammalian cells (14). *LKB1* regulates tight junction assembly and cell polarity through AMPK in mammalian cells (15, 16), and we have shown that *LKB1* suppresses tubulin polymerization by activating MARK microtubule-associated protein signaling (17). We have also reported that HCCs in *Lkb1*(+/-) mice metastasize to the lungs (10). However, the mechanisms by which *LKB1* suppresses cancer metastasis have not yet been explored. In this study, we have investigated the effect of *LKB1* on cell motility whose acquisition occurs in early metastasis (18).

The serine/threonine kinase PAK1 is known as a key regulator of cell motility, proliferation, differentiation, and survival (19). It can activate diverse signaling pathways, including LIM motif-containing protein kinase 1, mitogen-activated protein kinase (MAPK), and NF- κ B signaling (20). PAK1 interacts with the GTP-bound forms of Cdc42 or Rac, which cause PAK1 activation (21). In addition to activation by Cdc42/Rac, its activity is positively regulated also by other signaling molecules, including phosphoinositide 3-kinase (22), 3-phosphoinositide-dependent kinase-1 (23), and AKT (24).

PAK1 is overexpressed in various types of cancer, including breast (25, 26), colon (27), and liver (28) cancers. A high level of PAK1 expression is correlated with more aggressive tumor behaviors such as metastatic phenotype and advanced tumor stages in hepatocellular carcinomas (28) as well as in colorectal cancer (27). Consistently, overexpression of constitutively active mutant PAK1 (T423E) helps develop malignant mammary tumors in a transgenic mouse model (29). These results indicate that PAK1 plays a key role in carcinogenesis and cancer metastasis. Here, we present evidence that *LKB1* inhibits cell motility and PAK1-mediated signaling through direct phosphorylation of PAK1 at Thr¹⁰⁹ in the p21-binding domain.

* This work was supported by a grant-in-aid for scientific research (to M. M. T.), a grant-in-aid for young scientist (B) from the Ministry of Education, Culture, Sports, Science and Technology of Japan, and Littlefield-American Association for Cancer Research grants in metastatic colon cancer research (to M. M. T.).

[5] The on-line version of this article (available at <http://www.jbc.org>) contains supplemental "Experimental Procedures" and Fig. S1.

¹ To whom correspondence should be addressed: Dept. of Pharmacology, Graduate School of Medicine, Kyoto University, Yoshida-Konoé-cho, Sakyo-ku, Kyoto 605-8501, Japan. Tel.: 81-75-753-4391; Fax: 81-75-753-4402; E-mail: taketo@mfour.med.kyoto-u.ac.jp.

² The abbreviations used are: HCC, hepatocellular carcinoma; PAK1, p21-activated kinase-1; PBD, p21-binding domain; Adv, adenovirus; AMPK, AMP-activated protein kinase; STRAD, STE20-related adaptor pseudo-kinase; MARK, microtubule-associated protein/microtubule affinity-regulating kinase; siRNA, small interfering RNA; wt, wild-type; GST, glutathione S-transferase; HA, hemagglutinin; VASP, vasodilator-stimulated phosphoprotein.